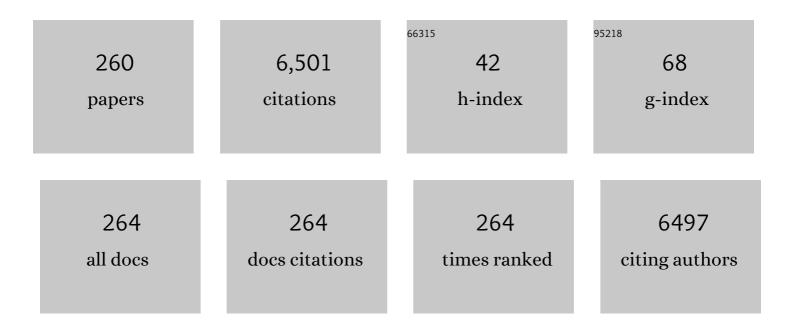
List of Publications by Year in descending order

Source: https://exaly.com/author-pdf/8121381/publications.pdf Version: 2024-02-01



#	Article	IF	CITATIONS
1	Intrinsic dependencies of <scp>CT</scp> radiomic features on voxel size and number of gray levels. Medical Physics, 2017, 44, 1050-1062.	1.6	428
2	A genome-based model for adjusting radiotherapy dose (GARD): a retrospective, cohort-based study. Lancet Oncology, The, 2017, 18, 202-211.	5.1	377
3	Non-invasive estimation of hyperthermia temperatures with ultrasound. International Journal of Hyperthermia, 2005, 21, 589-600.	1.1	189
4	The future of personalised radiotherapy for head and neck cancer. Lancet Oncology, The, 2017, 18, e266-e273.	5.1	168
5	Voxel size and gray level normalization of CT radiomic features in lung cancer. Scientific Reports, 2018, 8, 10545.	1.6	150
6	The 2019 mathematical oncology roadmap. Physical Biology, 2019, 16, 041005.	0.8	147
7	Phase III study of interstitial thermoradiotherapy compared with interstitial radiotherapy alone in the treatment of recurrent or persistent human tumors: A prospectively controlled randomized study by the radiation therapy oncology group. International Journal of Radiation Oncology Biology Physics, 1996, 34, 1097-1104.	0.4	138
8	Variability of Image Features Computed from Conventional and Respiratory-Gated PET/CT Images of Lung Cancer. Translational Oncology, 2015, 8, 524-534.	1.7	110
9	Abscopal Benefits of Localized Radiotherapy Depend on Activated T-cell Trafficking and Distribution between Metastatic Lesions. Cancer Research, 2016, 76, 1009-1018.	0.4	103
10	Measurement of DNA Damage after Exposure to Electromagnetic Radiation in the Cellular Phone Communication Frequency Band (835.62 and 847.74 MHz). Radiation Research, 1997, 148, 618.	0.7	102
11	VMAT QA: Measurement-guided 4D dose reconstruction on a patient. Medical Physics, 2012, 39, 4228-4238.	1.6	96
12	Measurement of DNA Damage and Apoptosis in Molt-4 Cells afterIn VitroExposure to Radiofrequency Radiation. Radiation Research, 2004, 161, 193-200.	0.7	93
13	A proliferation saturation index to predict radiation response and personalize radiotherapy fractionation. Radiation Oncology, 2015, 10, 159.	1.2	93
14	Noninvasive temperature estimation based on the energy of backscattered ultrasound. Medical Physics, 2003, 30, 1021-1029.	1.6	91
15	Reproducibility of F18â€FDG PET radiomic features for different cervical tumor segmentation methods, grayâ€level discretization, and reconstruction algorithms. Journal of Applied Clinical Medical Physics, 2017, 18, 32-48.	0.8	85
16	Measurement of DNA Damage after Exposure to 2450 MHz Electromagnetic Radiation. Radiation Research, 1997, 148, 608.	0.7	84
17	Development of Targeted Alpha Particle Therapy for Solid Tumors. Molecules, 2019, 24, 4314.	1.7	82
18	Chromosome Damage and Micronucleus Formation in Human Blood Lymphocytes ExposedIn Vitroto Radiofrequency Radiation at a Cellular Telephone Frequency (847.74 MHz, CDMA). Radiation Research, 2001, 156, 430-432.	0.7	81

#	Article	IF	CITATIONS
19	Cytogenetic Studies in Human Blood Lymphocytes ExposedIn Vitroto Radiofrequency Radiation at a Cellular Telephone Frequency (835.62 MHz, FDMA). Radiation Research, 2001, 155, 113-121.	0.7	78
20	Evaluation of Spatially Fractionated Radiotherapy (GRID) and Definitive Chemoradiotherapy With Curative Intent for Locally Advanced Squamous Cell Carcinoma of the Head and Neck: Initial Response Rates and Toxicity. International Journal of Radiation Oncology Biology Physics, 2010, 76, 1369-1375.	0.4	78
21	Experimentally studied dynamic dose interplay does not meaningfully affect target dose in VMAT SBRT lung treatments. Medical Physics, 2013, 40, 091710.	1.6	74
22	Initial evaluation of automated treatment planning software. Journal of Applied Clinical Medical Physics, 2016, 17, 331-346.	0.8	66
23	Proto-Oncogene mRNA Levels and Activities of Multiple Transcription Factors in C3H 10T 1/2 Murine Embryonic Fibroblasts Exposed to 835.62 and 847.74 MHz Cellular Phone Communication Frequency Radiation. Radiation Research, 1999, 151, 300.	0.7	64
24	Spatially Fractionated Radiation Induces Cytotoxicity and Changes in Gene Expression in Bystander and Radiation Adjacent Murine Carcinoma Cells. Radiation Research, 2012, 177, 751-765.	0.7	64
25	CT imaging features associated with recurrence in non-small cell lung cancer patients after stereotactic body radiotherapy. Radiation Oncology, 2017, 12, 158.	1.2	63
26	Clinical feasibility of TBI with helical tomotherapy. Bone Marrow Transplantation, 2011, 46, 929-935.	1.3	61
27	Study of 201 Non-Small Cell Lung Cancer Patients Given Stereotactic Ablative Radiation Therapy Shows Local Control Dependence on Dose Calculation Algorithm. International Journal of Radiation Oncology Biology Physics, 2014, 88, 1108-1113.	0.4	61
28	Simultaneous superficial hyperthermia and external radiotherapy: report of thermal dosimetry and tolerance to treatment. International Journal of Hyperthermia, 1999, 15, 251-266.	1.1	59
29	The Effect of 835.62 MHz FDMA or 847.74 MHz CDMA Modulated Radiofrequency Radiation on the Induction of Micronuclei in C3H 10T½ Cells. Radiation Research, 2002, 157, 506-515.	0.7	59
30	Pediatric Craniospinal Axis Irradiation With Helical Tomotherapy: Patient Outcome and Lack of Acute Pulmonary Toxicity. International Journal of Radiation Oncology Biology Physics, 2009, 75, 1155-1161.	0.4	58
31	Modeling of carbon fiber couch attenuation properties with a commercial treatment planning system. Medical Physics, 2008, 35, 4982-4988.	1.6	57
32	The Effect of Chronic Exposure to 835.62 MHz FDMA or 847.74 MHz CDMA Radiofrequency Radiation on the Incidence of Spontaneous Tumors in Rats. Radiation Research, 2003, 160, 143-151.	0.7	54
33	Microbeam Radiation Therapy Alters Vascular Architecture and Tumor Oxygenation and is Enhanced by a Galectin-1 Targeted Anti-Angiogenic Peptide. Radiation Research, 2012, 177, 804-812.	0.7	54
34	Imaging features from pretreatment <scp>CT</scp> scans are associated with clinical outcomes in nonsmallâ€cell lung cancer patients treated with stereotactic body radiotherapy. Medical Physics, 2017, 44, 4341-4349.	1.6	53
35	Measurement of DNA Damage in Mammalian Cells ExposedIn Vitroto Radiofrequency Fields at SARs of 3–5 W/kg. Radiation Research, 2001, 156, 328-332.	0.7	52
36	Temperature dependence of ultrasonic backscattered energy in motion compensated images. IEEE Transactions on Ultrasonics, Ferroelectrics, and Frequency Control, 2005, 52, 1644-1652.	1.7	52

#	Article	IF	CITATIONS
37	The radial transmission line as a broad-band shielded exposure system for microwave irradiation of large numbers of culture flasks. Bioelectromagnetics, 1999, 20, 65-80.	0.9	51
38	Precision of quantitative computed tomography texture analysis using image filtering. Medicine (United States), 2017, 96, e6993.	0.4	49
39	Measurement of DNA damage after acute exposure to pulsedâ€wave 2450 MHz microwaves in rat brain cells by two alkaline comet assay methods. International Journal of Radiation Biology, 2004, 80, 11-20.	1.0	48
40	Radiation-Induced Alterations in Mitochondria of the Rat Heart. Radiation Research, 2014, 181, 324.	0.7	48
41	A method for <i>a priori</i> estimation of best feasible <scp>DVH</scp> for organsâ€atâ€risk: Validation for head and neck <scp>VMAT</scp> planning. Medical Physics, 2017, 44, 5486-5497.	1.6	48
42	Evaluation of Parameters of Oxidative Stress afterIn VitroExposure to FMCW- and CDMA-Modulated Radiofrequency Radiation Fields. Radiation Research, 2004, 162, 497-504.	0.7	45
43	The Evolution of Tumour Composition During Fractionated Radiotherapy: Implications for Outcome. Bulletin of Mathematical Biology, 2018, 80, 1207-1235.	0.9	45
44	Integrating Mathematical Modeling into the Roadmap for Personalized Adaptive Radiation Therapy. Trends in Cancer, 2019, 5, 467-474.	3.8	43
45	Nonthermal Effects of Radiofrequency-Field Exposure on Calcium Dynamics in Stem Cell-Derived Neuronal Cells: Elucidation of Calcium Pathways. Radiation Research, 2008, 169, 319-329.	0.7	40
46	Head and Neck Tumor Control Probability: Radiation Dose–Volume Effects in Stereotactic Body Radiation Therapy for Locally Recurrent Previously-Irradiated Head and Neck Cancer: Report of the AAPM Working Group. International Journal of Radiation Oncology Biology Physics, 2021, 110, 137-146.	0.4	37
47	Micronuclei in the peripheral blood and bone marrow cells of rats exposed to 2450 MHz radiofrequency radiation. International Journal of Radiation Biology, 2001, 77, 1109-1115.	1.0	36
48	Radiosensitization of heat resistant human tumour cells by 1 hour at 41.1°C and its effect on DNA repair. International Journal of Hyperthermia, 2002, 18, 385-403.	1.1	36
49	3-D in vitro estimation of temperature using the change in backscattered ultrasonic energy. IEEE Transactions on Ultrasonics, Ferroelectrics, and Frequency Control, 2010, 57, 1724-1733.	1.7	36
50	Modelling millimetre wave propagation and absorption in a high resolution skin model: the effect of sweat glands. Physics in Medicine and Biology, 2011, 56, 1329-1339.	1.6	36
51	Simultaneous delivery of electron beam therapy and ultrasound hyperthermia using scanning reflectors: a feasibility study. International Journal of Radiation Oncology Biology Physics, 1995, 31, 893-904.	0.4	35
52	Radiofrequency Electromagnetic Fields Have No Effect on the In Vivo Proliferation of the 9L Brain Tumor. Radiation Research, 1999, 152, 665.	0.7	35
53	37, 2351-2358.	1.6	35
54	Comprehensive evaluation of the highâ€resolution diode array for SRS dosimetry. Journal of Applied Clinical Medical Physics, 2019, 20, 13-23.	0.8	35

#	Article	IF	CITATIONS
55	Radiofrequency Electromagnetic Fields do not Alter the Cell Cycle Progression of C3H 10T and U87MG Cells. Radiation Research, 2001, 156, 786-795.	0.7	34
56	Gene Expression does not Change Significantly in C3H 10T½ Cells after Exposure to 847.74 CDMA or 835.62 FDMA Radiofrequency Radiation. Radiation Research, 2006, 165, 626-635.	0.7	34
57	<i>In vivo</i> change in ultrasonic backscattered energy with temperature in motion-compensated images. International Journal of Hyperthermia, 2008, 24, 389-398.	1.1	34
58	Investigating multi-radiomic models for enhancing prediction power of cervical cancer treatment outcomes. Physica Medica, 2018, 46, 180-188.	0.4	34
59	Immune interconnectivity of anatomically distant tumors as a potential mediator of systemic responses to local therapy. Scientific Reports, 2018, 8, 9474.	1.6	34
60	Present and future technology for simultaneous superficial thermoradiotherapy of breast cancer. International Journal of Hyperthermia, 2010, 26, 699-709.	1.1	33
61	Transfection of human tumour cells with Mre11 siRNA and the increase in radiation sensitivity and the reduction in heat-induced radiosensitization. International Journal of Hyperthermia, 2004, 20, 157-162.	1.1	32
62	Modelling heat-induced radiosensitization: clinical implications. International Journal of Hyperthermia, 2004, 20, 201-212.	1.1	31
63	The Heat-Shock Factor is not Activated in Mammalian Cells Exposed to Cellular Phone Frequency Microwaves. Radiation Research, 2005, 164, 163-172.	0.7	31
64	Melanocortin 1 Receptor–Targeted α-Particle Therapy for Metastatic Uveal Melanoma. Journal of Nuclear Medicine, 2019, 60, 1124-1133.	2.8	31
65	Forecasting Individual Patient Response to Radiation Therapy in Head and Neck Cancer With a Dynamic Carrying Capacity Model. International Journal of Radiation Oncology Biology Physics, 2021, 111, 693-704.	0.4	31
66	Experimental and numerical determination of SAR distributions within culture flasks in a dielectric loaded radial transmission line. IEEE Transactions on Biomedical Engineering, 2000, 47, 202-208.	2.5	30
67	Measurements of Alkali-Labile DNA Damage and Protein–DNA Crosslinks after 2450 MHz Microwave and Low-Dose Gamma IrradiationIn Vitro. Radiation Research, 2004, 161, 201-214.	0.7	30
68	A Simulation Model for Ultrasonic Temperature Imaging Using Change in Backscattered Energy. Ultrasound in Medicine and Biology, 2008, 34, 289-298.	0.7	30
69	Cardiac Inflammation after Local Irradiation Is Influenced by the Kallikrein-Kinin System. Cancer Research, 2012, 72, 4984-4992.	0.4	30
70	Simultaneous radiotherapy and superficial hyperthermia for high-risk breast carcinoma: A randomised comparison of treatment sequelae in heated versus non-heated sectors of the chest wall hyperthermia. International Journal of Hyperthermia, 2012, 28, 583-590.	1.1	29
71	Effects of Late Administration of Pentoxifylline and Tocotrienols in an Image-Guided Rat Model of Localized Heart Irradiation. PLoS ONE, 2013, 8, e68762.	1.1	29
72	Monte Carlo comparison of superficial dose between flattening filter free and flattened beams. Physica Medica, 2014, 30, 503-508.	0.4	28

#	Article	IF	CITATIONS
73	A Tocotrienol-Enriched Formulation Protects against Radiation-Induced Changes in Cardiac Mitochondria without Modifying Late Cardiac Function or Structure. Radiation Research, 2015, 183, 357.	0.7	28
74	Predicting Patient-Specific Radiotherapy Protocols Based on Mathematical Model Choice for Proliferation Saturation Index. Bulletin of Mathematical Biology, 2018, 80, 1195-1206.	0.9	28
75	A compact shielded exposure system for the simultaneous long-term UHF irradiation of forty small mammals: I. Electromagnetic and environmental design. Bioelectromagnetics, 1998, 19, 459-468.	0.9	27
76	Dead or alive? Autofluorescence distinguishes heat-fixed from viable cells. International Journal of Hyperthermia, 2009, 25, 355-363.	1.1	27
77	Effects of local irradiation combined with sunitinib on early remodeling, mitochondria, and oxidative stress in the rat heart. Radiotherapy and Oncology, 2016, 119, 259-264.	0.3	27
78	Energy deposition processes in biological tissue: Nonthermal biohazards seem unlikely in the ultra-high frequency range. Bioelectromagnetics, 2001, 22, 97-105.	0.9	26
79	Components of a hyperthermia clinic: Recommendations for staffing, equipment, and treatment monitoring. International Journal of Hyperthermia, 2014, 30, 1-5.	1.1	26
80	SURLAS: A new clinical grade ultrasound system for sequential or concomitant thermoradiotherapy of superficial tumors: Applicator description. Medical Physics, 2005, 32, 230-240.	1.6	25
81	Retrospective Evaluation of Pediatric Cranio-Spinal Axis Irradiation Plans with the Hi-ART Tomotherapy System. Technology in Cancer Research and Treatment, 2007, 6, 355-360.	0.8	25
82	A dosimetric comparison of volumetric modulated arc therapy with step-and-shoot intensity modulated radiation therapy for prostate cancer. Practical Radiation Oncology, 2015, 5, 11-15.	1.1	24
83	Proliferation saturation index in an adaptive Bayesian approach to predict patient-specific radiotherapy responses. International Journal of Radiation Biology, 2019, 95, 1421-1426.	1.0	24
84	Accounting for reconstruction kernel-induced variability in CT radiomic features using noise power spectra. Journal of Medical Imaging, 2017, 5, 1.	0.8	24
85	Monte Carlo Study of Radiation Dose Enhancement by Gadolinium in Megavoltage and High Dose Rate Radiotherapy. PLoS ONE, 2014, 9, e109389.	1.1	24
86	Altered Calcium Dynamics Mediates P19-Derived Neuron-Like Cell Responses to Millimeter-Wave Radiation. Radiation Research, 2009, 172, 725-736.	0.7	23
87	Advanced Small Animal Conformal Radiation Therapy Device. Technology in Cancer Research and Treatment, 2017, 16, 45-56.	0.8	23
88	A comparison of theoretical and experimental ultrasound field distributions in canine muscle tissue in vivo. Ultrasound in Medicine and Biology, 1992, 18, 81-95.	0.7	22
89	Ultrasound power deposition model for the chest wall. Ultrasound in Medicine and Biology, 1999, 25, 1275-1287.	0.7	22
90	On the Assumption of Negligible Heat Diffusion during the Thermal Measurement of a Nonuniform Specific Absorption Rate. Radiation Research, 1999, 152, 312.	0.7	22

#	Article	IF	CITATIONS
91	Pretreatment CT and ¹⁸ Fâ€FDG PETâ€based radiomic model predicting pathological complete response and locoâ€regional control following neoadjuvant chemoradiation in oesophageal cancer. Journal of Medical Imaging and Radiation Oncology, 2021, 65, 102-111.	0.9	22
92	An ultrasound system for simultaneous ultrasound hyperthermia and photon beam irradiation. International Journal of Radiation Oncology Biology Physics, 1996, 36, 1189-1200.	0.4	21
93	Expression of the Proto-oncogeneFosafter Exposure to Radiofrequency Radiation Relevant to Wireless Communications. Radiation Research, 2005, 164, 420-430.	0.7	21
94	The effects of 41ŰC hyperthermia on the DNA repair protein, MRE11, correlate with radiosensitization in four human tumor cell lines. International Journal of Hyperthermia, 2007, 23, 343-351.	1.1	21
95	Effects of radiation on the epidermal growth factor receptor pathway in the heart. International Journal of Radiation Biology, 2013, 89, 539-547.	1.0	21
96	Sensitivity of Image Features to Noise in Conventional and Respiratory-Gated PET/CT Images of Lung Cancer: Uncorrelated Noise Effects. Technology in Cancer Research and Treatment, 2017, 16, 595-608.	0.8	21
97	Simplified model and measurement of specific absorption rate distribution in a culture flask within a transverse electromagnetic mode exposure system. Bioelectromagnetics, 1999, 20, 183-193.	0.9	20
98	Practical quantification of image registration accuracy following the <scp>AAPM TG</scp> â€132 report framework. Journal of Applied Clinical Medical Physics, 2018, 19, 125-133.	0.8	20
99	CTâ€based radiomic features to predict pathological response in rectal cancer: A retrospective cohort study. Journal of Medical Imaging and Radiation Oncology, 2020, 64, 444-449.	0.9	20
100	Thermal contribution of compact bone to intervening tissue-like media exposed to planar ultrasound. Physics in Medicine and Biology, 2004, 49, 869-886.	1.6	19
101	Monitoring the effect of mild hyperthermia on tumour hypoxia by Cu-ATSM PET scanning. International Journal of Hyperthermia, 2006, 22, 93-115.	1.1	19
102	Conductive interstitial thermal therapy device for surgical margin ablation: <i>In vivo</i> verification of a theoretical model. International Journal of Hyperthermia, 2007, 23, 477-492.	1.1	19
103	The number of genes changing expression after chronic exposure to Code Division Multiple Access or Frequency DMA radiofrequency radiation does not exceed the false-positive rate. Proteomics, 2006, 6, 4739-4744.	1.3	18
104	Thermoradiotherapy is underutilized for the treatment of cancer. Medical Physics, 2006, 34, 1-4.	1.6	18
105	Potential for power deposition conformability using reflected-scanned planar ultrasound. International Journal of Hyperthermia, 1996, 12, 723-736.	1.1	17
106	MicroPET-compatible, small animal hyperthermia ultrasound system (SAHUS) for sustainable, collimated and controlled hyperthermia of subcutaneously implanted tumours. International Journal of Hyperthermia, 2004, 20, 32-44.	1.1	17
107	Cross-validation of two commercial methods for volumetric high-resolution dose reconstruction on a phantom for non-coplanar VMAT beams. Radiotherapy and Oncology, 2014, 110, 558-561.	0.3	17
108	Roles of Sensory Nerves in the Regulation of Radiation-Induced Structural and Functional Changes in the Heart. International Journal of Radiation Oncology Biology Physics, 2014, 88, 167-174.	0.4	17

#	Article	IF	CITATIONS
109	The importance of dead material within a tumour on the dynamics in response to radiotherapy. Physics in Medicine and Biology, 2020, 65, 015007.	1.6	17
110	An investigation of penetration depth control using parallel opposed ultrasound arrays and a scanning reflector. Journal of the Acoustical Society of America, 1997, 101, 1734-1741.	0.5	16
111	Acoustic field prediction for a single planar continuous-wave source using an equivalent phased array method. Journal of the Acoustical Society of America, 1997, 102, 2734-2741.	0.5	16
112	Experimental assessment of power and temperature penetration depth control with a dual frequency ultrasonic system. Medical Physics, 1999, 26, 810-817.	1.6	16
113	Magnetic resonance biomarkers in radiation oncology: The report of AAPM Task Group 294. Medical Physics, 2021, 48, e697-e732.	1.6	16
114	Dynamics-Adapted Radiotherapy Dose (DARD) for Head and Neck Cancer Radiotherapy Dose Personalization. Journal of Personalized Medicine, 2021, 11, 1124.	1.1	16
115	Aperture size to therapeutic volume relation for a multielement ultrasound system: Determination of applicator adequacy for superficial hyperthermia. Medical Physics, 1993, 20, 1399-1409.	1.6	15
116	Numerical and <i>in vitro</i> evaluation of temperature fluctuations during reflected-scanned planar ultrasound hyperthermia. International Journal of Hyperthermia, 1998, 14, 367-382.	1.1	15
117	Compact shielded exposure system for the simultaneous long-term UHF irradiation of forty small mammals II. Dosimetry. Bioelectromagnetics, 1999, 20, 81-93.	0.9	15
118	In regard to Vasanathan et al. (Int J Radiat Oncol Biol Phys 2005;61:145–153). International Journal of Radiation Oncology Biology Physics, 2005, 63, 644.	0.4	15
119	Quantification of the skin sparing effect achievable with high-energy photon beams when carbon fiber tables are used. Radiotherapy and Oncology, 2009, 93, 147-152.	0.3	15
120	Severe, short-duration (0–3 min) heat shocks (50–52°C) inhibit the repair of DNA damage. International Journal of Hyperthermia, 2010, 26, 67-78.	1.1	15
121	Effects of quantum noise in 4D-CT on deformable image registration and derived ventilation data. Physics in Medicine and Biology, 2013, 58, 7661-7672.	1.6	15
122	A three phase model to investigate the effects of dead material on the growth of avascular tumours. Mathematical Modelling of Natural Phenomena, 2020, 15, 22.	0.9	15
123	A Method to Determine the Coincidence of MRI-Guided Linac Radiation and Magnetic Isocenters. Technology in Cancer Research and Treatment, 2019, 18, 153303381987798.	0.8	14
124	A reflected-scanned ultrasound system for external simultaneous thermoradiotherapy. IEEE Transactions on Ultrasonics, Ferroelectrics, and Frequency Control, 1996, 43, 441-449.	1.7	13
125	A Novel Technique for Image-Guided Local Heart Irradiation in the Rat. TCRT Express, 2014, 13, 593-603.	1.5	13
126	Development and testing of a database of NIH research funding of AAPM members: A report from the AAPM Working Group for the Development of a Research Database (WGDRD). Medical Physics, 2017, 44, 1590-1601.	1.6	13

#	Article	IF	CITATIONS
127	The impact of ultrasonic parameters on chest wall hyperthermia. International Journal of Hyperthermia, 2000, 16, 523-538.	1.1	12
128	Experience with a small animal hyperthermia ultrasound system (SAHUS): report on 83 tumours. Physics in Medicine and Biology, 2005, 50, 5127-5139.	1.6	12
129	Conductive Interstitial Thermal Therapy (CITT) Device Evaluation in VX2 Rabbit Model. Technology in Cancer Research and Treatment, 2007, 6, 235-245.	0.8	12
130	Dosimetric Comparison of Helical Tomotherapy and Linac-IMRT Treatment Plans for Head and Neck Cancer Patients. Medical Dosimetry, 2010, 35, 264-268.	0.4	12
131	Impact of dose on lung ventilation change calculated from 4D-CT using deformable image registration in lung cancer patients treated with SBRT. Journal of Radiation Oncology, 2015, 4, 265-270.	0.7	12
132	Validation of a <scp>GPU</scp> â€Based 3D dose calculator for modulated beams. Journal of Applied Clinical Medical Physics, 2017, 18, 73-82.	0.8	12
133	A hybrid volumetric dose verification method for singleâ€isocenter multipleâ€target cranial SRS. Journal of Applied Clinical Medical Physics, 2018, 19, 651-658.	0.8	12
134	Biological Optimization in Volumetric Modulated Arc Radiotherapy for Prostate Carcinoma. International Journal of Radiation Oncology Biology Physics, 2012, 82, 1292-1298.	0.4	11
135	Evaluation of the ΔV 4D CT ventilation calculation method using <i>in vivo</i> xenon CT ventilation data and comparison to other methods. Journal of Applied Clinical Medical Physics, 2016, 17, 550-560.	0.8	11
136	Doppler signals observed during high temperature thermal ablation are the result of boiling. International Journal of Hyperthermia, 2010, 26, 586-593.	1.1	10
137	Voxel-Based Dose Reconstruction for Total Body Irradiation With Helical TomoTherapy. International Journal of Radiation Oncology Biology Physics, 2012, 82, 1575-1583.	0.4	10
138	A Monte Carlo Method for Determining the Response Relationship between Two Commonly Used Detectors to Indirectly Measure Alpha Particle Radiation Activity. Molecules, 2019, 24, 3397.	1.7	10
139	Localized versus regional hyperthermia: Comparison of xenotransplants treated with a small animal ultrasound system and waterbath limb immersion. International Journal of Hyperthermia, 2005, 21, 271-281.	1.1	9
140	HSP27 phosphorylation increases after 45°C or 41°C heat shocks but not after non-thermal TDMA or GSM exposures. International Journal of Hyperthermia, 2006, 22, 507-519.	1.1	9
141	Conductive interstitial thermal therapy (CITT) inhibits recurrence and metastasis in rabbit VX2 carcinoma model. International Journal of Hyperthermia, 2009, 25, 446-454.	1.1	9
142	Pretreatment CT and PET Radiomics Predicting Rectal Cancer Patients in Response to Neoadjuvant Chemoradiotherapy. Reports of Practical Oncology and Radiotherapy, 2021, 26, 29-34.	0.3	9
143	AAPM Task Group 241: A medical physicist's guide to MRIâ€guided focused ultrasound body systems. Medical Physics, 2021, 48, e772-e806.	1.6	9
144	Treatment delivery software for a new clinical grade ultrasound system for thermoradiotherapy. Medical Physics, 2005, 32, 3246-3256.	1.6	8

#	Article	IF	CITATIONS
145	Feasibility of concurrent treatment with the scanning ultrasound reflector linear array system (SURLAS) and the helical tomotherapy system. International Journal of Hyperthermia, 2008, 24, 377-388.	1.1	8
146	PET imaging of heat-inducible suicide gene expression in mice bearing head and neck squamous cell carcinoma xenografts. Cancer Gene Therapy, 2009, 16, 161-170.	2.2	8
147	Validation of an improved helical diode array and dose reconstruction software using TGâ€244 datasets and stringent dose comparison criteria. Journal of Applied Clinical Medical Physics, 2016, 17, 163-178.	0.8	8
148	Heat-induced SIRT1-mediated H4K16ac deacetylation impairs resection and SMARCAD1 recruitment to double strand breaks. IScience, 2022, 25, 104142.	1.9	8
149	Ultrasound field estimation method using a secondary source-array numerically constructed from a limited number of pressure measurements. Journal of the Acoustical Society of America, 2000, 107, 3259-3265.	0.5	7
150	Is wax equivalent to tissue in electron conformal therapy planning? A Monte Carlo study of material approximation introduced dose difference. Journal of Applied Clinical Medical Physics, 2013, 14, 92-101.	0.8	7
151	Normalization of Ventilation Data from 4D-CT to Facilitate Comparison between Datasets Acquired at Different Times. PLoS ONE, 2013, 8, e84083.	1.1	7
152	A robust power deposition scheme for tumors with large counter-current blood vessels during hyperthermia treatment. Applied Thermal Engineering, 2015, 89, 897-907.	3.0	7
153	Lipophilicity Determines Routes of Uptake and Clearance, and Toxicity of an Alpha-Particle-Emitting Peptide Receptor Radiotherapy. ACS Pharmacology and Translational Science, 2021, 4, 953-965.	2.5	7
154	Measuring temporal stability of positron emission tomography standardized uptake value bias using long-lived sources in a multicenter network. Journal of Medical Imaging, 2018, 5, 1.	0.8	7
155	Spatially fractionated (GRID) therapy for large and bulky tumors. The Journal of the Arkansas Medical Society, 2009, 105, 263-5.	0.1	7
156	Lung Dose for Minimally Moving Thoracic Lesions Treated With Respiration Gating. International Journal of Radiation Oncology Biology Physics, 2010, 77, 285-291.	0.4	6
157	An alternating focused ultrasound system for thermal therapy studies in small animals. Medical Physics, 2011, 38, 1877-1887.	1.6	6
158	SonoKnife: Feasibility of a lineâ€focused ultrasound device for thermal ablation therapy. Medical Physics, 2011, 38, 4372-4385.	1.6	6
159	Measurementâ€guided volumetric dose reconstruction for helical tomotherapy. Journal of Applied Clinical Medical Physics, 2015, 16, 302-321.	0.8	6
160	Deep Feature Stability Analysis Using CT Images of a Physical Phantom across Scanner Manufacturers, Cartridges, Pixel Sizes, and Slice Thickness. Tomography, 2020, 6, 250-260.	0.8	6
161	A concentric-ring equivalent phased array method to model fields of large axisymmetric ultrasound transducers. IEEE Transactions on Ultrasonics, Ferroelectrics, and Frequency Control, 1999, 46, 830-841.	1.7	5
162	Influence of the SURLAS applicator on radiation dose distributions during simultaneous thermoradiotherapy with helical tomotherapy. Physics in Medicine and Biology, 2008, 53, 2509-2522.	1.6	5

EDUARDO G MOROS

#	Article	IF	CITATIONS
163	Fiducial markers coupled with 3D PET/CT offer more accurate radiation treatment delivery for locally advanced esophageal cancer. Endoscopy International Open, 2017, 05, E496-E504.	0.9	5
164	Analysis of the 2017 American Society for Radiation Oncology (ASTRO) Research Portfolio. International Journal of Radiation Oncology Biology Physics, 2019, 103, 297-304.	0.4	5
165	Unlocking a closed system: dosimetric commissioning of a ring gantry linear accelerator in a multivendor environment. Journal of Applied Clinical Medical Physics, 2021, 22, 21-34.	0.8	5
166	Maintaining dosimetric quality when switching to a Monte Carlo dose engine for head and neck volumetricâ€modulated arc therapy planning. Journal of Applied Clinical Medical Physics, 2022, 23, e13572.	0.8	5
167	High dose-rate induced temperature artifacts: Thermometry considerations for simultaneous interstitial thermoradiotherapy. International Journal of Radiation Oncology Biology Physics, 1994, 30, 399-403.	0.4	4
168	A two-parameter method for the estimation of ultrasound-induced temperature artifacts. International Journal of Hyperthermia, 1999, 15, 187-202.	1.1	4
169	Proliferation Saturation Index Predicts Oropharyngeal Squamous Cell Cancer Gross Tumor Volume Reduction to Prospectively Identify Patients for Adaptive Radiation Therapy. International Journal of Radiation Oncology Biology Physics, 2016, 94, 903.	0.4	4
170	Study of Image Qualities From 6D Robot–Based CBCT Imaging System of Small Animal Irradiator. Technology in Cancer Research and Treatment, 2017, 16, 811-818.	0.8	4
171	Biodistribution and Multicompartment Pharmacokinetic Analysis of a Targeted α Particle Therapy. Molecular Pharmaceutics, 2020, 17, 4180-4188.	2.3	4
172	Responses to the 2018 and 2019 "One Big Discovery―Question: ASTRO Membership's Opinions on the Most Important Research Question Facing Radiation Oncology…Where Are We Headed?. International Journal of Radiation Oncology Biology Physics, 2021, 109, 38-40.	0.4	4
173	Electromagnetic and thermal characterization of an UHF-applicator for concurrent irradiation and high resolution non-perturbing optical microscopy of cells. Bioelectromagnetics, 2006, 27, 593-601.	0.9	3
174	Electromagnetic and thermal evaluation of an applicator specialized to permit highâ€resolution nonâ€perturbing optical evaluation of cells being irradiated in the Wâ€band. Bioelectromagnetics, 2010, 31, 140-149.	0.9	3
175	Fiducial-based image-guided radiotherapy for whole breast irradiation. Journal of Radiation Oncology, 2013, 2, 185-190.	0.7	3
176	Dose-mass inverse optimization for minimally moving thoracic lesions. Physics in Medicine and Biology, 2015, 60, 3927-3937.	1.6	3
177	A multi-user networked database for analysis of clinical and temperature data from patients treated with simultaneous radiation and ultrasound hyperthermia. International Journal of Hyperthermia, 1999, 15, 419-426.	1.1	2
178	Intensity-Modulated Radiotherapy for Craniospinal Irradiation: Target Volume Considerations, Dose Constraints and Competing Risks: In Regard to Parker etÂal. (Int J Radiat Oncol Biol Phys) Tj ETQq0 0 0 rgBT /Over	lock 10 Ti	5 20 137 Td
179	Static jaw collimation settings to minimize radiation dose to normal brain tissue during stereotactic radiosurgery. Medical Dosimetry, 2012, 37, 391-395.	0.4	2

180Assessment of intact cervix motion using implanted fiducials in patients treated with helical
tomotherapy with daily MVCT positioning. Journal of Radiation Oncology, 2013, 2, 323-329.0.72

#	Article	IF	CITATIONS
181	Mathematical Formulation of DMH-Based Inverse Optimization. Frontiers in Oncology, 2014, 4, 331.	1.3	2
182	Motion as perturbation. II. Development of the method for dosimetric analysis of motion effects with fixed-gantry IMRT. Medical Physics, 2014, 41, 061704.	1.6	2
183	Technical Note: Motionâ€perturbation method applied to dosimetry of dynamic MLC target tracking—A proofâ€ofâ€concept. Medical Physics, 2015, 42, 6147-6151.	1.6	2
184	Role of the bradykinin B2 receptor in a rat model of local heart irradiation. International Journal of Radiation Biology, 2015, 91, 634-642.	1.0	2
185	Open access journals benefit authors from more affluent institutions. Medical Physics, 2016, 43, 5265-5267.	1.6	2
186	Integral dose based inverse optimization objective function promises lower toxicity in head-and-neck. Physica Medica, 2018, 54, 77-83.	0.4	2
187	Radiomic assessment of the progression of acoustic neuroma after gamma knife stereotactic radiosurgery. Journal of Solid Tumors, 2019, 9, 1.	0.1	2
188	SU-C-BRB-01: Spatially Fractionated Radiation Therapy (GRID) Using a TomoTherapy Unit. Medical Physics, 2011, 38, 3369-3369.	1.6	2
189	<title>Use of A-scan for penetration control during dual-frequency ultrasound thermal therapy of superficial tissues overlaying bone and lung</title> . , 1999, , .		1
190	Ventilation Series Similarity: A Study for Ventilation Calculation Using Deformable Image Registration and 4DCT to Avoid Motion Artifacts. Contrast Media and Molecular Imaging, 2017, 2017, 1-7.	0.4	1
191	Responses to the 2017 "1 Million Gray Question†ASTRO Membership's Opinions on the Most Important Research Question Facing Radiation Oncology. International Journal of Radiation Oncology Biology Physics, 2018, 102, 249-250.	0.4	1
192	Composite Pretreatment CT and 18F-FDG PET Radiomic-Based Prediction of Pathological Response of Rectal Cancer Patients Treated with Neoadjuvant Chemoradiotherapy. International Journal of Radiation Oncology Biology Physics, 2019, 105, E177.	0.4	1
193	The ASTRO Research Portfolio: Where Do We Go From Here?. International Journal of Radiation Oncology Biology Physics, 2019, 103, 308-309.	0.4	1
194	SU-FF-T-403: Target Failure and Beam-On Load in Helical Tomotherapy. Medical Physics, 2006, 33, 2138-2138.	1.6	1
195	SU-FF-J-160: Spatially Fractionated Radiation Therapy (GRID) On Implanted Tumors Using a Small Animal Conformal Radiation Therapy System. Medical Physics, 2009, 36, 2514-2514.	1.6	1
196	SU-FF-T-609: Dose Summation Technology for Radiation Therapy Facilities Equipped with Heterogeneous Planning and Delivery Systems. Medical Physics, 2009, 36, 2664-2665.	1.6	1
197	TU-C-BRD-03: An Integrated Robotic-Based Irradiation System for Small Animal Research. Medical Physics, 2009, 36, 2720-2720.	1.6	1
198	WE-E-220-04: Focused Ultrasound Ablation of Tumour Hypoxic Tissue of Small Animals under PET and MRI Guidance. Medical Physics, 2011, 38, 3824-3824.	1.6	1

#	Article	IF	CITATIONS
199	SU-E-J-187: Evaluation of the Effects of Dose on 4DCT-Calculated Lung Ventilation. Medical Physics, 2012, 39, 3695-3696.	1.6	1
200	SUâ€Eâ€Tâ€479: Skin Dose from Flattening Filter Free Beams: A Monte Carlo Investigation. Medical Physics, 2012, 39, 3815-3815.	1.6	1
201	Fiducial markers vs. PET/CT for esophageal cancer GTV delineation for radiotherapy treatment planning using a standard SUV threshold and background uptake method Journal of Clinical Oncology, 2016, 34, 70-70.	0.8	1
202	Multicenter survey of PET/CT protocol parameters that affect standardized uptake values. Journal of Medical Imaging, 2017, 5, 1.	0.8	1
203	Stability of deep features across CT scanners and field of view using a physical phantom. , 2018, , .		1
204	Superficial and peripheral dose in compensator-based FFF beam IMRT. Journal of Applied Clinical Medical Physics, 2017, 18, 151-156.	0.8	1
205	Superficial and peripheral dose in compensatorâ€based FFF beam IMRT. Journal of Applied Clinical Medical Physics, 2017, 18, 151-156.	0.8	1
206	Multi-Angle Switched HIFU: A New Ultrasound Device for Controlled Non-Invasive Induction of Small Spherical Ablation Zones—Simulation and Ex-Vivo Results. , 2009, , .		0
207	Thermal treatment planning for SonoKnife focused-ultrasound thermal treatment of head and neck cancers. Proceedings of SPIE, 2011, , .	0.8	0
208	Dual thermal ablation modality of solid tumors in a mouse model. , 2011, , .		0
209	Experimental characterization of a SonoKnife applicator. , 2011, , .		0
210	Computed effects of sweat gland ducts on the propagation of 94 GHz waves in skin. Proceedings of SPIE, 2011, , .	0.8	0
211	SonoKnife for ablation of neck tissue: In vivo verification of a computer layered medium model. International Journal of Hyperthermia, 2012, 28, 698-705.	1.1	0
212	X-RAY COLLIMATOR DESIGN USING MONTE CARLO SIMULATIONS. Biomedical Engineering - Applications, Basis and Communications, 2013, 25, 1350054.	0.3	0
213	On the dose to a moving target in stereotactic ablative body radiotherapy to lung tumors. Journal of Physics: Conference Series, 2017, 777, 012027.	0.3	0
214	SU-FF-T-320: Simple Acoustic Beam Model for Thermoradiotherapy Implemented in An Open Source Treatment Planning Research System. Medical Physics, 2005, 32, 2024-2024.	1.6	0
215	SU-FF-T-317: Options for SURLAS Design Modification Due to the Impact of Ultrasound Nonlinear Propagation. Medical Physics, 2005, 32, 2023-2023.	1.6	0
216	WE-D-224C-07: A Comprehensive Patient-Specific IMRT Quality Assurance Procedure On Hi-Art Tomotherapy® Unit. Medical Physics, 2006, 33, 2250-2250.	1.6	0

#	Article	IF	CITATIONS
217	SU-FF-T-336: Patient-Specific QA in MLC-Based GRID Therapy. Medical Physics, 2007, 34, 2479-2479.	1.6	0
218	WEâ€Câ€M100Fâ€09: Dosimetric Comparison of Linacâ€IMRT and Helical Tomotherapy (HT) for Head and Neck Cancer. Medical Physics, 2007, 34, 2593-2593.	1.6	0
219	SU-GG-J-170: Small Animal Conformal Radiation Therapy Device. Medical Physics, 2008, 35, 2718-2718.	1.6	0
220	SUâ€GCâ€Tâ€539: Carbon Fiber Couch Effect On Skin Doses as a Function of Photon Energy. Medical Physics, 2008, 35, 2848-2849.	1.6	0
221	SUâ€GCâ€Jâ€151: Potential Lung Dose Reduction for Minimallyâ€Moving Lung Lesions. Medical Physics, 2008, 35 2714-2714.	⁵ ,1.6	0
222	SUâ€GCâ€Jâ€160: Radiation Enclosure Shielding Calculations for a Laboratoryâ€Based Small Animal Conformal Radiation Therapy Device. Medical Physics, 2008, 35, 2716-2716.	1.6	0
223	TH-C-304A-03: MVCT Auto-Contouring for Adpative Radiation Therapy. Medical Physics, 2009, 36, 2803-2803.	1.6	Ο
224	SU-FF-T-152: Comparison Between Fixed Gantry Angle Intensity Modulated Radiotherapy and Intensity Modulated Arc Therapy for Head-And-Neck Cancers. Medical Physics, 2009, 36, 2555-2555.	1.6	0
225	TH-C-BRC-08: Integration of Cone Beam CT Imaging and a Small Animal Conformal RT Device Using a 6DOF Robotic Arm. Medical Physics, 2009, 36, 2799-2799.	1.6	0
226	SU-FF-T-208: Dose Verification for Total Marrow Irradiation Using HELICAL TOMOTHERAPY Planned Adaptive. Medical Physics, 2009, 36, 2568-2568.	1.6	0
227	SU-FF-J-124: When Do We Need to Consider Motion Management During Treatment of Mobile Lesions?. Medical Physics, 2009, 36, 2505-2505.	1.6	Ο
228	SU-FF-T-248: Quality Assurance for Total Marrow Irradiation (TMI) Using Helical Tomotherapy. Medical Physics, 2009, 36, 2577-2578.	1.6	0
229	SU-GG-I-178: Numerical Simulations of the SonoKnife's Acoustic Edge. Medical Physics, 2010, 37, 3142-3142.	1.6	0
230	SUâ€GGâ€Tâ€294: Quality Assurance for Small SRS Photon Field Using LUCY Phantom on BrainLab Iplan. Medical Physics, 2010, 37, 3253-3253.	1.6	0
231	WEâ€Dâ€201Câ€04: SonoKnife — Feasibility of Lineâ€Focused Ultrasound for Thermal Ablation. Medical Physic 2010, 37, 3432-3432.	^{S,} 1.6	0
232	SUâ€GGâ€Tâ€534: The Impact of Linac Static Jaw Setting on Dose Output from Small Field SRS/SRT Using an Addâ€On Microâ€Multileaf Collimator. Medical Physics, 2010, 37, 3310-3310.	1.6	0
233	SUâ€GGâ€Tâ€⊋99: A Digital QA Solution Using 2D Ion Chamber Array. Medical Physics, 2010, 37, 3254-3254.	1.6	0
234	SU-GG-T-10: Deformable Model Based Dose Reconstruction for Total Body Irradiation with Helical TomoTherapy. Medical Physics, 2010, 37, 3185-3185.	1.6	0

#	Article	IF	CITATIONS
235	SU-GC-I-105: Ultrafast Deformable Image Registration for Potential Adaptive Total Body Irradiation Therapy Using Helical TomoTherapy. Medical Physics, 2010, 37, 3125-3125.	1.6	0
236	Abstract 1570: Thermal ablation improves oxygenation in remaining viable tumor. , 2011, , .		0
237	SU-E-T-537: A Dosimetric Study of Gafchromic EBT2 Film for Small Field Size Stereotactic Radiosurgery QA. Medical Physics, 2011, 38, 3612-3612.	1.6	0
238	SU-E-T-318: Using Monte Carlo in the Design of Small Animal Irradiator Collimators. Medical Physics, 2011, 38, 3560-3561.	1.6	0
239	WE-E-220-03: SonoKnife: Development, Testing and Treatment Planning. Medical Physics, 2011, 38, 3824-3824.	1.6	0
240	SU-E-I-15: CBCT Using a Robotic-Arm Based Small Animal Irradiation System. Medical Physics, 2011, 38, 3398-3399.	1.6	0
241	SU-E-T-802: Dosimetric Examination and Verification of Megavoltage Computed Tomography (MVCT) Based IMRT Treatment Planning with Helical TomoTherapy. Medical Physics, 2011, 38, 3675-3675.	1.6	0
242	SU-E-T-848: Dose Mass - Based IMRT Inverse Planning for Radiotherapy of Thoracic Cancer. Medical Physics, 2011, 38, 3686-3686.	1.6	0
243	SU-E-T-312: Development of a Rat Model of Radiation-Induced Heart Disease Using SACRTD. Medical Physics, 2011, 38, 3559-3559.	1.6	0
244	SU-E-T-572: Dose Mass Histogram (DMH) versus Dose Volume Histogram (DVH) for SBRT and Craniospinal Patients: What Can We Learn?. Medical Physics, 2011, 38, 3621-3621.	1.6	0
245	SU-E-J-167: Optimal Number of Respiratory Phases in 4D PET for Radiotherapy Planning: Motion-Simulated Phantom Study. Medical Physics, 2012, 39, 3691-3691.	1.6	0
246	SU-E-T-553: Dose-Mass Vs. Dose-Volume Optimization: A Phantom Study. Medical Physics, 2012, 39, 3832-3833.	1.6	0
247	TH-C-137-12: Comparison of Dose-Volume and Dose-Mass Inverse Optimization in NSCLC. Medical Physics, 2013, 40, 535-535.	1.6	0
248	SU-E-T-239: Implementation of QA Procedures and Their Effect On the Radiation Treatment Delivery Error Rate Over a 12 Year Period. Medical Physics, 2013, 40, 259-259.	1.6	0
249	SU-E-J-69: Normalization of Ventilation Data From 4D-CT for Comparison Before and After Treatment. Medical Physics, 2013, 40, 165-165.	1.6	0
250	SU-E-J-203: Texture Analysis of 3D and 4D PET/CT Images of Lung Cancer. Medical Physics, 2013, 40, 198-198.	1.6	0
251	TH-A-137-07: Local Control Differences for SBRT Lung Patients Planned with Pencil Beam Vs. Collapsed Cone Convolution Algorithms. Medical Physics, 2013, 40, 518-518.	1.6	Ο
252	SU-E-J-66: Effects of Noise in 4D-CT On Deformable Image Registration and Derived Ventilation Data. Medical Physics, 2013, 40, 165-165.	1.6	0

#	Article	IF	CITATIONS
253	Equivalent phased array methods to predict acoustic fields of planar and focused ultrasound transducers. Journal of the Acoustical Society of America, 1997, 102, 3086-3086.	0.5	0
254	Abstract A18: A systems biology approach to predict immunotherapy augmented abscopal effects. , 2015, , .		0
255	Abstract A19: Systems biology approach predicts the diagnostic value of T effector: T regulatory cell ratio in clinical response to combined radiation/immunotherapy of high-risk soft tissue sarcoma. , 2015, , .		0
256	WE-FG-BRA-10: Radiodosimetry of a Novel Alpha Particle Therapy Targeted to Uveal Melanoma: Absorbed Dose to Organs in Mice. Medical Physics, 2016, 43, 3825-3826.	1.6	0
257	4DCT-Derived Ventilation Distribution Reproducibility Over Time. Communications in Computer and Information Science, 2017, , 56-66.	0.4	0
258	Big Data Approaches to Improve Stereotactic Body Radiation Therapy (SBRT) Outcomes. Advances in Medical Diagnosis, Treatment, and Care, 2018, , 94-113.	0.1	0
259	Temperature Feedback Control for Hyperthermia of Chest Wall Volumes With Dual-Frequency Ultrasound. , 1999, , .		0
260	Model for Ultrasonic Heating of Chest Wall Recurrences. , 1998, , .		0